ANALYSIS OF THE INDUSTRIAL SHEET METAL FORMING PROCESS USING THE FORMING LIMIT DIAGRAM (FLD) THROUGH COMPUTER SIMULATION AS INTEGRATED TOOL IN CAR BODY DEVELOPMENT

Gleiton Luiz Damoulis
Edson Gomes
Gilmar Ferreira Batalha
Laboratório de Engenharia de Fabricação - Escola Politécnica da Universidade de São Paulo – Depto of Mechatronics & Mechanical Systems Engineering - Av. Prof. Mello Moraes, 2231, 05508.970 - S. Paulo, SP - BRAZIL. Fone 00 55 11 30915763 - e-mail: gilmar.batalha@poli.usp.br

Abstract: *New market requirements have becoming more persistent through the introduction of new technologies that can lead the actual vehicle designs to reach very high safety standards, reduce of weight (improvements on fuel consumption, emissions and performance trends), world class quality levels at reasonable production costs and schedule timing for product development, due new design features and mainly the introduction of new technological materials for a so called Lightweight Car Body Concept. A new generation of simulation software's based on explicit or implicit Finite Element Method (FEM) are becoming more affordable and are increasing their reliability in the presented results. The question is, how can these software support the process/product development engineer in the choose of the right body-in-white component design, blank and tool geometries, the right process parameters and moreover the right material choose, mainly due the market introduction of many new technological steels families for car body construction in the last years. As an example, in the car body-in-white development, the design of body panels can be supported effectively by the use of the Forming Limit Diagram (FLD), through the computer simulation of the sheet metal forming process with the FEM. This work describes how an explicit finite element program can be applied to lay out industrial deep drawing processes, accomplished by the use of the FLD methodology and the updating procedure for the model data and the computational process. The main part of the paper discusses simulation applied skills and explains in an example of industrial process how the use of the FLD can helps to improve the interpretation of the simulation and in the choice of the best steel.*
Keywords: *sheet metal forming, forming limit diagram, computer simulation, finite element*.

1. INTRODUCTION

To reach the new market requirement targets for the automotive body development, process integration since the early concept development phases until the start of production, must provide a streamlined scalable environment that encompasses every step in the process from early design feasibility to the process final validation. High safety standards, the high reduction of weight that improves fuel consumption, emissions and performance trends, a world class quality at reasonable production costs and schedule timing are changing the development chain in the automotive industry. Mainly regarding automotive lightweight construction based on the use of lightweight materials, meaning that building materials of low specific density and high-strength can be used, automotive engineers and designers are being challenged everyday, through the introduction of many new materials for their applications. And for this, new design aims and methodologies should be developed [Batalha, Damoulis & Schwarzwald, 2003]. Vehicle body-in-white (BIW) complains usually complex geometry, irregular pressed parts. Forming these blanks is normally a combination

of deep drawing and stretching and bending. A detailed analysis and judging of the forming process with conventional processes requires a lot of energy for most cases. Process simulation in the forming technique with the Finite Element Method (FEM) is an efficient and low cost tool for simulation of the forming process before tool production. During all stages of the forming process before tool production the FEM simulation enables a detailed judging of forming material, the optimal tool form and the process the control. A variety of effects such as plastically orthotropy and strain rate dependence of the material as well as different friction conditions in the contact area sheet-tool, are describable and corresponding friction conditions are put at disposal by the programs. In this sense a consequent use of stamping simulation enables: Saving of development time by means of securing the development course and to reduce costs as well as a quality improvement of stamping parts by means of optimization of the drawing process, process parameter, material choice, blank and forming steps. The effects of some of these parameters on the forming process window are resumed on the Figure 1. The present investigation wants to demonstrate which degree of agreement can be achieved between analysis and test, mainly with the aim of a Forming Limit Diagram (FLD) analysis for some practical use of FEM simulation in the automotive industry as: Sheet thickness distribution, Equivalent plastics strains, Material flow, Failure (tearing and wrinkling), FLD quality contour plot, Blank and forming geometry and Punch and holder force.

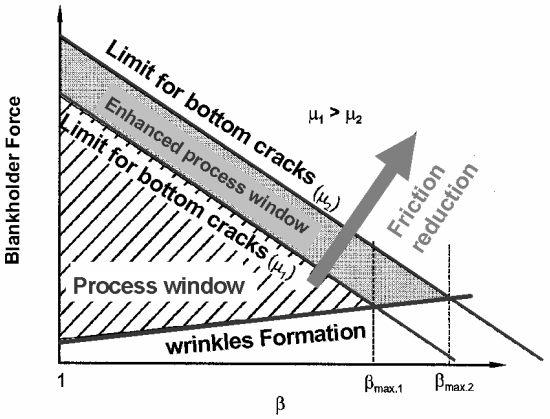

Figure 1. Process window for metal sheet forming process: failure modes and influences.

2. FEATURES, ADVANTAGES & DISADVANTAGES OF FEM IN METAL FORMING

The simulation of metal forming process is one of the major challenges for non-linear FE-Analysis, as all non-linearity concerning geometry with large rotations and large displacements, material with large strains and contact with friction are involved in a large extend. Dynamic explicit finite elements codes are widely used in most of the automotive industries, as they are very robust and efficient for large-scale problems like this. In such codes the systems of equations are integrated in an explicit-dynamic method, which, in contrast to an implicit approach, does not involve the solution of complex, coupled non-linear equations.

2.1 The speed issue

According to [Haug et al, 1991 and Makinouchi, 2001], a potential drawback with explicit solutions is their inherent incapacity to furnish one-shoot static solution to structural problems. This is due to the fact that they operate on the dynamic equation:

$$M\ddot{x} = F \tag{1}$$

Where M is the (diagonal) mass matrix $\ddot{x}$ is the acceleration in the structural degrees of freedom and F are internal resisting forces and external loads. Together with the conditionally stable central difference dynamic solution algorithm, velocity and displacements can be calculated at discrete time intervals, the stable step size of which depends on the smallest travel time of elastic stress waves between points of a discrete model (speed of sound in the material). Also in most practical

cases the punch velocity can safely be increased by substantial factors without the inertia effects of the moved sheet particles to significantly affect the results. Preliminary investigations showed that punch velocities might reach 15-20 m/s and more, before the effect of inertia will have an influence in the principal stamping results. Another simple means to reduce unwanted inertia effects is to apply loads and punch velocities not suddenly, but by ramping up the load with carefully chosen functions of time, thus reducing spurious high frequency response effects from the outset. Judicious application of internal and external damping can also reduce such effects and can lead to stable quasi-static asymptotically solutions.

2.2. Contact and Friction

Among the most important enhancements in a crash simulation program needed for the successful simulation of stamping processes, are the adequate descriptions of the material behavior and the complex contact/friction phenomena between the blank (sheet) and the tools (punch, blank holders and dies). Basic Coulomb friction will not adequately describe the dependence of the friction coefficients on normal pressure, sliding velocity etc. Contact between the tools and sheet is identified with efficient search algorithms, and contact forces are calculated with a penalty force method that is equivalent to the mechanical system. [Damoulis & Batalha, 2003]. Together with a robust algorithm, a penalty K based contact is of a one sided searching master-slave type and contact damping C proportional to the relative velocity of both contact areas that allows for complex problems with many elements to be treated efficiently and reliably [Heath et al. 1993].

2.2.1 Friction Laws

When an accurate description of material behavior appears necessary for successful stamping simulation an accurate description of the friction phenomena has equal importance, because the nature of the tangent forces created by friction between the blank and the tools may be the decisive factor for the manufacturability of a stamped component. In more enhanced models, the friction coefficient should be related to external variables such as mean contact pressure, relative speed of the tooling and sheet, the lubricant viscosity and surface roughness. This approach models a Stribeck curve behavior for the friction coefficient and could be useful to regard some effects like the rheological properties of the lubricant and the influence of normal pressure on the friction behavior [Azuchima et al, 1998] as well as the surface topography [Batalha et al, 2000 & 2001]. Friction laws relate a tangent contact stress t, to normal contact pressures, via a friction coefficient μ, which may also depend on contact normal pressure s_n, the tangent sliding velocity v and on the lubricant, the temperature, the sliding distance, the sliding direction and the sheet deformation [Damoulis & Batalha, 2003].

2.3 Material Constitutive Equations

For the accuracy of the simulation results it becomes very important to put the more exact possible boundary conditions in the program. In this sense the following inputs must be informed: at one hand the plastic behavior and at the other hand the contact and friction conditions, as well as the geometric data. The plastic behavior influences the blank in two ways: a pronounced isotropic hardening helps to achieve uniformly strained drawn parts, as through the Lankford coefficient distribution the anisotropic hardening controls the direction of the plastic flow. In terms of material laws the plastic behavior is specified by the yield curve and the yield locus.

2.3.1 The yield curve

The yield curve could be obtained by tensile, compression or torsion tests; stress-strain curves obtained in the uniaxial tensile test generally does not support realistic numerical simulations. In this sense, it becomes very useful when possible to use multi-axial tests, in the simplest situation bi-axial results. Larger deformations ranges can be obtained by combination of tests, specifically for sheet metal the combinations of the tensile test and the bulge test as well as tensile and shear test using Miyauchi specimen have been reported and also recommended some care with the strain hardening behavior, as it is one of the most influencing parameter on the failure [Hora et al. 2001].

2.3.2 The yield locus

The accuracy of the yield locus determination has the same importance of the yield stress-strain curve for the improvement of the FEM simulations [Berg e Hora, 2000]. The material of the sheets is usually highly ductile steel, which is rendered an isotropic, due to the cold work during the rolling process or pre-stresses. It is common to specify the yield locus using r-values; specifications based on the texture are more rarely used [Thieme, 1995], figure 2. Among several models describing the yield locus shape stands established for example the non-quadratic functions proposed by Hill (1948, 1979, 1990) [Hill 1948 and 1979] and the Barlat-Lian functions (1979, 1990) [Damoulis, 2005] as well as the Isotropy Center Translation Theory, For the scope of this paper, the yield locus shape can be described according to Hill (1948) the anisotropy plasticity can either be considered stationary (von Mises / Hill criteria) or evolutionary (e.g., ICT Isotropy Center Translation Theory). Both formulations are incorporated into the program code and outlined below, as well as simple work hardening and strain rate assumptions

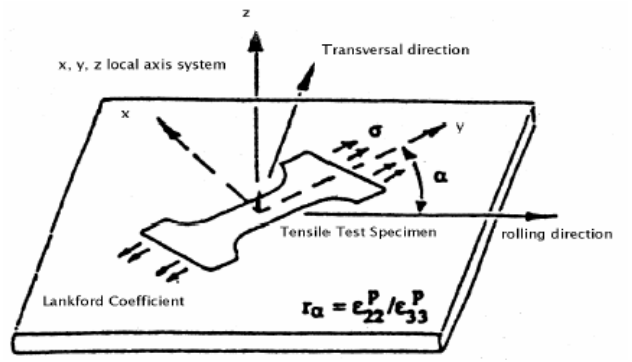

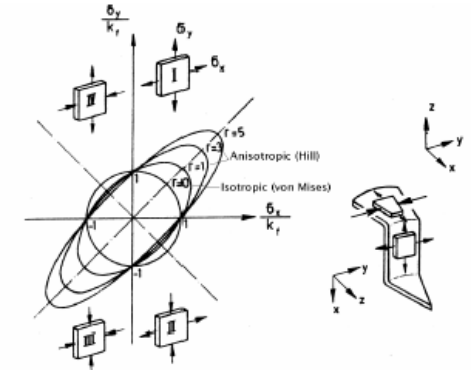

Figure 2. Anisotropy and Yield locus for different r values.

2.3.3 Von Mises and Hill Type Plasticity Laws

If the sheet material is assumed to exhibit planar and normally orthotropic plastic behavior, then the yield function for plane stress states can be expressed as a Hill type criterion as follows in eq. 4:.

$$F(\sigma_{22}-\sigma_{33})^2 + G(\sigma_{33}-\sigma_{11})^2 + H(\sigma_{11}-\sigma_{22})^2 + 2L\sigma_{23}^{\ 2} + 2M\sigma_{31}^{\ 2} + 2N\sigma_{12}^{\ 2} = 2Y^2 \quad (4)$$

2.3.3.1 Orthotropic Material

i) Hill Coefficient for Lankford ratio=0:

$$\sigma = \frac{1}{\sqrt{2}}[2(2+F-G)\sigma_{22}^{\ 2} + 2\sigma_{11}^{\ 2} - 2(2-G)\sigma_{11}\sigma_{22} + N\sigma_{12}^{\ 2}]^{1/2} \quad (5)$$

ii) Hill Coefficient for Lankford ratio=1

$$\sigma = \frac{1}{\sqrt{P(R+1)}}[R(P+1)\sigma_{22}^{\ 2} + P(R+1)\sigma_{11}^{\ 2} - 2RP\sigma_{11}\sigma_{22} + (2Q+1)(R+P)\sigma_{12}^{\ 2}]^{1/2} \quad (6)$$

2.3.3.2 Normal Anisotropy Material (Lankford > 0)

$$\sigma = \frac{1}{\sqrt{RL+1}}[(RL+1)(\sigma_{22}^{\ 2}+\sigma_{11}^{\ 2}) - 2RL\sigma_{11}\sigma_{22}(2Q+1)(R+P)\sigma_{12}^{\ 2}]^{1/2} \quad (7)$$

Where :

$$Lankford = \mathrm{RL} = \frac{1}{n}\sum_{i=1}^{n} RLi \quad (8)$$

2.3.3.3 Normal Isotropy Material (Lankford = 0)

$$\sigma = [(\sigma_{22}{}^2 + \sigma_{11}{}^2) + (\sigma_{11} + \sigma_{22})^2 + 3\sigma_{12}{}^2]^{1/2} \qquad (9)$$

This means a *von Mises* isotropic behavior: *Lankford* ratio = 0, where 1, 2 and 3 are the axial, transverse and normal directions of a test coupon cut out at a angle ?*a* with respect to the rolling (or pre stress) direction; *P*, *Q* and *R* are *Lankford* coefficients (r_a) , where:

$$r_\alpha = \varepsilon_{22}(\alpha)/\varepsilon_{33}(\alpha) \qquad (10)$$

for angles a = 90°, 45° e 0° respectively (figure 4), which are determinate by a multi-axial tension test; e_{22} and e_{33} are experimentally measured transverse and normal (plastic) strains; s_{11}, s_{12} and s_{22} are in plane normal and shear stresses of the material, (*F*,*G*,*H*,*L*,*M*,*N*) are constant parameters and?s_{ij} is the stress tensor. *Hill* formulate his theory assuming that the material is homogeny in the three orthogonal directions x, y and z , and all the properties related to this material has double symmetry equivalent (the planes $x-y$, $y-z$ and $z-x$ are from symmetry). For a laminated steel sheet, one can assumes x on the laminate direction, y is the transverse direction to the laminate direction on the sheet plane and z to the normal plane related to the sheet thickness. *Hill'*s theory assumes that on these three directions the yielding resistances are quite different, but those are equal on tensile and compression stresses. Therefore some premises can be assumed, and the *Hill'*s criteria for anisotropy can be write on the form:

$$2f(\sigma_{ij}) = F(\sigma_y - \sigma_z)^2 + G(\sigma_z - \sigma_x)^2 + H(\sigma_x - \sigma_y)^2 + 2L\tau_{yz}^2 + 2M\tau_{zx}^2 + 2N\tau_{xy}^2 = 1 \qquad (11)$$

Note that if *F=G=H* and *L=M=N=3F*, we have the criteria of *von Mises*. The constants F, G and H can be obtained from a uniaxial tensile test. Considering a test in the *x* direction, and assuming that X will be the yield stress, one can be write $s_x = X, s_y = s_z = t_{ij} = 0$, than the equation (11) will become:

$$(G+H)X^2 = 1 \qquad (12)$$

Similar to this, if *Y* and *Z* are the yield stresses on the y and z directions respectively, then we have:

$$X^2 = \frac{1}{G+H} \qquad (13)$$

$$Y^2 = \frac{1}{H+F} \qquad (14)$$

$$Z^2 = \frac{1}{F+G} \qquad (15)$$

That will lead us to the following results:

$$2F = \frac{1}{X^2} + \frac{1}{Z^2} - \frac{1}{X^2} \qquad (16)$$

$$2G = \frac{1}{Z^2} + \frac{1}{X^2} - \frac{1}{Y^2} \qquad (17)$$

$$2H = \frac{1}{X^2} + \frac{1}{Y^2} - \frac{1}{Z^2} \qquad (18)$$

There is also a problem within these relations, because it is not possible to measure the resistance *Z* on the sheet metal thickness direction. Before to solve this problem, it is necessary to calculate *L*, *M* and *N*. Using perhaps a general *Hook's* law described such as:

$$e = \frac{1}{E}[s_1 - n(s_2 + s_3)] \tag{19}$$

Applying (19) on the equation (11), through a differential we have the following laws describing the yielding phenomenal to each direction:

$$de_x = dl\left[H(s_x - s_y) + G(s_x - s_z)\right],\ de_{xy} = de_{zy} = dlLt_{yz} \tag{20}$$

$$de_y = dl\left[F(s_y - s_z) + H(s_y - s_x)\right],\ de_{zx} = de_{xz} = dlLt_{zx} \tag{21}$$

$$de_z = dl\left[F(s_z - s_y) + G(s_z - s_x)\right],\ de_{xy} = de_{yx} = dlLt_{xy} \tag{22}$$

In the equations (21), (22) and (23), also a hypothesis of a constant volume is respect, or:

$$de_x + de_y + de_z = 0 \tag{24}$$

Considering the uniaxial test on the x direction, and replacing $s_x = X$, $s_y = s_z = 0$ on (21), (22) and (23), we can respectively write:

$$de_x = dl(H + G)X \tag{25}$$

$$de_y = dl(H)X \tag{26}$$

$$de_z = dl(G)X \tag{27}$$

As the quotient of the deformations for the x direction on the uniaxial test, we have the anisotropic coefficient expressed as:

$$R = R_0 = (de_y / de_z) \tag{28}$$

That leads us to the relation:

$$R = \frac{H}{G} \tag{29}$$

On the same way, for the y direction, defined that for the relation of $P = R_{90} = (de_x / de_z)$, with $s_y = Y$ and for $s_x = s_z = 0$, the result will be:

$$P = \frac{H}{F} \tag{30}$$

With the equations (25), (26) e (27) and for the execution of a uniaxial test for the directions x and y, measuring R, P, X e Y, using equations (16), (17) e (18), one can estimates the yield stresses on the z,Z direction, as

$$\frac{Z^2}{X^2} = \frac{(G + F)}{(F + G)} = \frac{(1/R) + 1}{(1/R) + (1/P)} \tag{31}$$

$$Z = X\sqrt{P(1 + R)}/(P + R) \tag{32}$$

A plasticity algorithm based on these criterions have been incorporated to the FEM-Program, incorporating the additional assumption that Y is a function of the effective plastic strain e^p and the plastic strain tensor ε_{ij}^p:

$$e^P = \sqrt{(2/3 e_{ij}^P e_{ij}^P)} \tag{33}$$

The value Y can be defined either through experimental points or with the *Krupokowski* formula:

$$Y = K(e^P + e_0)^n \tag{34}$$

Where K is the hardening factor, e_0 is the offset strain and n is the hardening exponent in *Krupkowski's* formula. These Material parameters can be obtained through fitting from measured uniaxial stress-strains curves. An alternative formation of evaluative orthotropic (or anisotropic) plastic behavior, well adapted to sheet steel material, is the recent phenomenological theory of *Isotropy Center Translation* (ICT). According to *Maziliu* et al (1990), this theory of anisotropy plasticity, the deviatoric invariant of the isotropic yield function translate independently from each other in stress space, producing translations and distortions of the yield surface, following any pre-deformation. The distortion is due to the anisotropy induced by the appearance of texture in the microscopic polycrystalline aggregate, [Damoulis G. and Batalha G., 2003].

2.4 The Forming Limit Diagram (FLD)

The physical properties of the metallic sheet can considerably change, through mainly depending on the material properties, alloy, thermal treatments presents and hardening effect on this. Searching for a specific material, engineers are looking for a compromise between the functional requirements on the sheet metal part design and the stamping properties of this material. For instance, a deep analysis of the influent factors on the material drawing properties should be carried on, such as:

- the reach of high levels of strains without appearance of necking effect; overlapping occurrence (*buckles and wrinkles*);	- the level of shear stresses on the deformation plan for no occurrence of cracks or tearing;
- the maximum level of compression stresses on he deformation plane, for no material	- quality aspects of the surface after the part removal from the tooling.
- The uniform strain distribution;	

For a specific material, some important properties are very decisive during a drawing operation, such as the *Young Modulus* E and the *Poisson's* coefficient n. In order to obtain high strain rates during a drawing operation and for the uniform distribution of these, a material choice clearly should be decisive mainly about the hardening exponent n, the deformation sensitivity rate m and the anisotropy coefficient g_a (*Lankford's* ratio) defined on the equation (10).

2.4.1 Graphic representation on the FLD

Group of points represented within (e_1, e_2) in a sheet metal on mechanical processing can be associated or related to some kind of possible occurrences in a general diagram. Those points can be determined using also experimental tests, such as *Swift (1952), Fukui (1958), Keeler e Goodwin (1968)* and *Nakazima (1968).* These representation is so called the forming limit diagram (FLD) and should be take as a support to the analyses of a specifically material conformability, as represented on the figure 3. For the use on Finite element analysis, the FLD can be displayed in a 2D window, where the same results are displayed onto the structure analyzed. This contains points, which represent the shell elements and the external faces of bricks in the space of main strains or stresses (minor in abscissa, major in ordinate). These main values are found again in the strain/stress isocolors. For a given material it is possible to use a FLD, which separates the diagram into two zones: above the curve, the points correspond to elements in rupture. From this FLD, the user can:

- Group the elements per "zones" of diagram, a zone corresponding to a part of the diagram delimited by forming Limit Curves (FLC);
- Group the elements per "zones" of quality (strains diagram only).

In the figure 3 we can identify the marked zones on the circles: Zone 1: **cracks**. Points located above the forming limit curve (failure). Zone 2: **excessive thinning**. Points located between the forming limit curve and the same curve decreased of 10% of the curve value at x=0. Zone 3: **safe zone** (good parts). Zone 4: **insufficient stretching**. Points located inside the circle whose center is the origin and whose radius value is 0.002. Zone 5: **wrinkling tendency**. Points located above the

y=-x straight line and under the y=((-1-Rm)/Rm)*x straight line (Rm = Average Lankford coefficient). Zone 6: **strong wrinkling tendency**. Points located under the y=-x straight line. To quantify the "risk of rupture" per element, by measuring the distance **d** of the point associated to the element to the FLC selected as reference. A negative value corresponds to a point below the curve, positive to a point above. For the strains diagram, *d* corresponds to the distance in Y (constant minor strain) to the FLC, as represented on the figure 4.

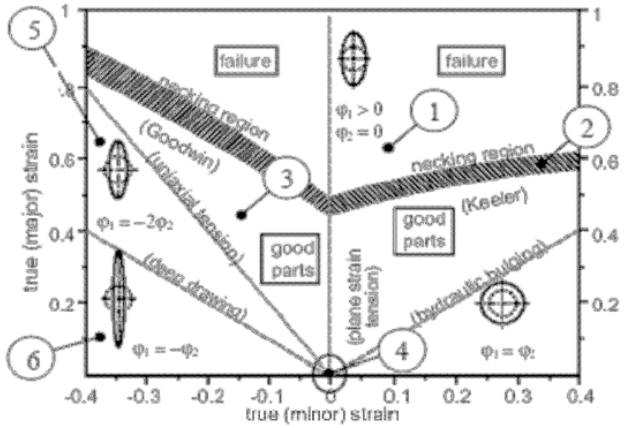

Figure 3. Representation of possible sheet metal drawing occurrences in a true (major) strain (j_1) and true minor strain diagram (j_2).

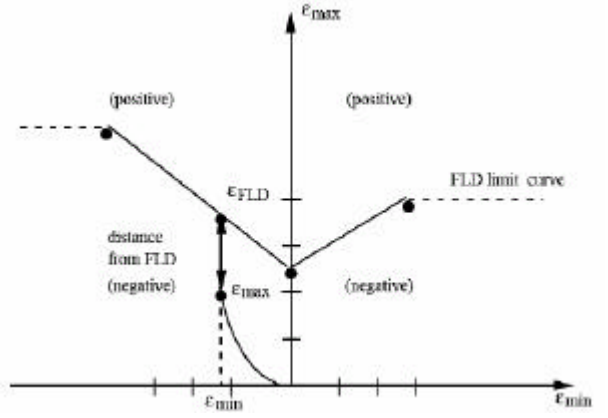

Figure 4. Representation of FLD according to a FEM analysis.

3. EXAMPLE OF INDUSTRIAL APPLICATION

To evaluate simulation accuracy by comparison with experimental results of the industry the calculations have been performed with the FEM program PAM-STAMP 2K© which can treat complicated geometry with acceptable run times. The considered parts exhibited here is a body-in-white quarter internal side panel. Quantities used for comparison were in each case the shape of the deformed sheet, thickness and strain distributions as well as the forming force history.

3.1 Model Discretisation

To perform this calculation, a side quarter panel from a small car was taken and in the critical deep-drawing area (figure 5) and a FEM model from the geometry were made. The sheet metal dimension in this case is 250x150mm. For the sheet material an St1405 was defined, which is an usual material for deep drawing applications in the automotive industry for such parts. The material identification data is represented in the Table 1.

Table.1 Sheet metal properties

Mechanical properties		*Lankford Coefficient*	
E [GPa]	210	P	1,8
n	0,30	Q	1,5
K	0,5673	R	2,3
e_0	0,0073	m_{db}	0,1
n	0,264	Sheet Thickness [mm]	1,00

A friction coefficient of 0,1 has been used, according to the *Coulomb's* law and an equivalent draw bead model has been defined. The chosen loads are 1200 kN for the holder and 3000 kN for the punch. The tool is considered as a rigid body and it was described as 11048 elements for the die, 1219 elements for the holder and 10023 elements for the punch. To achieve the results, it was decided to perform the calculations in two different forming phases. The first one demonstrates the behavior of the sheet after the contact between die/holder and the second one until the punch has reached the die top.

3.2 Forming Stages

To describe the calculation models, the PAM-STAMP 2K© program has been used. It was prepared an offset from the die and holder model (figure 7a). The holder is forced and damped to ground to prevent undesired dynamic oscillations and the holder velocity is increased to a maximum of 2m/s. The sheet initial phase was performed with initially with 1287 shell elements and finished the phase 2 with 20592 elements, (initially only after 3.3 hours CPU usage time performance), finishing this phase after 4 hours. Note that the adaptative mesh only was performed only at almost at the finish of the first phase, saving CPU time, according to the necessity of local improvement, for the output of the phase 2. For the forming phase 2, after the blank holder action, a second model was prepared within the output date from the phase 1, considering in this model the punch driving into the die (figure 7b). For representation reasons the model (b) is showed opened, but we consider the blank holder in contact with the pre-formed sheet. The punch velocity in the phase 2 is increased to a maximum of 10 m/s. In this calculation, 16.5 hours of CPU were used on total and the automatic mesh refinement program has allowed to the over limit of 36000 elements to perform phase 2, mainly in the areas were the large strains were detected, improving the local results, (diagram on figure 6).

3.3 Simulation Results

After simulation on the phase 1 (figure 6 and 7a) it can be seen that the figure demonstrates the basic capacity of the simulation of point of failure at the wrinkling of the sheet under the blank holder, owing to low holder pressure. Here it can be can also seen the undesired direction of the pre-formed sheet against the punch that can lead us to an undesired behavior of the sheet inside the tool. In the figure 8 it can be evaluate the thickness distribution over the part.

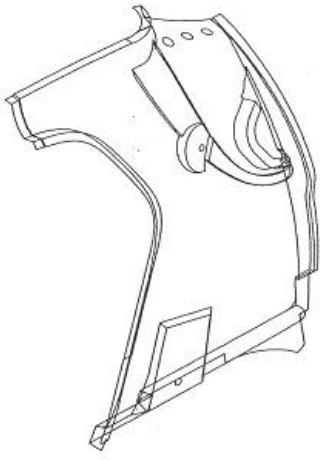

Figure 5. Body-in-white quarter side panel.

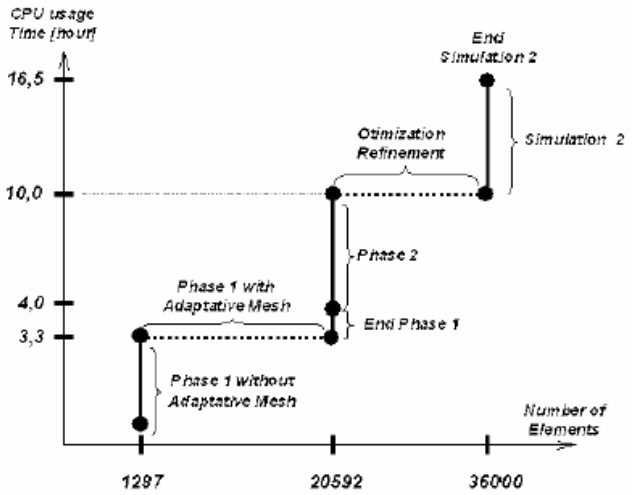

Figure 6. Simulation process representation diagram of CPU usage in [hours] related to the number of shell elements used.

A very important criterion for this evaluation will be the Forming Limit Diagram (FLD), where every finite element with its respective principal strain is represented. All the points over the limit forming represent a tearing point during the drawing process. In the fig.8 the thickness distribution is displayed. In two areas the minimal thickness decrease under 0,48 mm, what takes a high probability to tear. In these local a mesh refinement were necessary to improve the local analysis accuracy (figure 6, from 20592 up to 36000 elements).

3.3.1 Forming Limit Diagram Results

As showed on chapter 5, and on the same way as an experiment, the PAM-STAMP 2K© software can be used as a virtual device for the FLD plotting, using a specific technique (constant minor strain plot) to create a representative plot inside the FLC, in a certain way where can be possible to verify if a certain point (or element) attempts also to a certain drawing criteria.

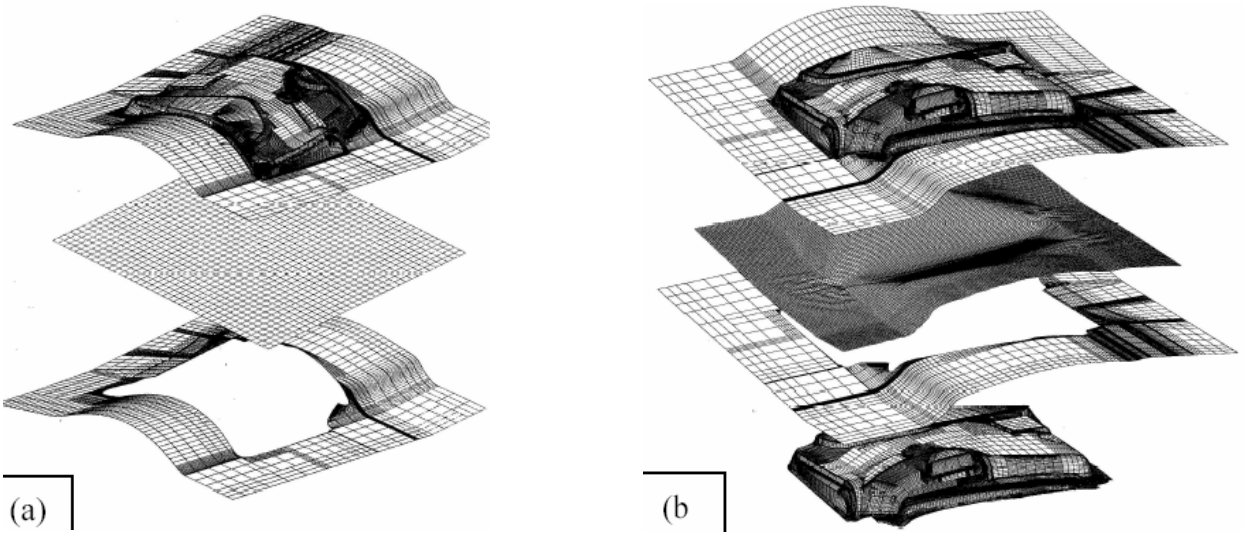

Figure 7. Forming phases 1 (a) and 2 (b) discretization FE models.

The definition of a criteria for the representation of these points n inside the FLC is based on the definition of a criteria, if the major plastic strain of a element exceeds the major specified elongation of this element, a so called $e_{p\_\max}$, or if the incremental step for a element is under the time step $\Delta t_{\min}$ minimum required (a specified time step). For stamping simulations purposes, using a material definition MATERIAL_TYPE_100 (a typical PAM-STAMP card definition), an element will be eliminated if the actual thickness rate (calculated on a certain time step) get under the starting thickness (*blank* thickness), reducing this to a specified minimum rate or, also if those major strains for an element exceed the specified limits in the FLD (limit curves, material dependent). If a FLC is defined, the program will also to plot on the diagram the distance of this point to the limit curves. The relative distance of a point $(e_{\min}, e_{\max})$ on the FLD, in relation to a specified limit curve can be calculated through:

$$d = (e_{\max} - e_{FLD}) / e_{FLD} \tag{35}$$

where e_{FLD} is the limit value on the elongation curve $e_{\min}$, as in the figure 8. In the figure 9 we have the representation of the maximum strains over the part geometry in reference to the *blank* thickness reduction, focusing on the critical stamped area and in the fig. 10 the referent forming diagram is displayed to determine the critical points where the plastic strains are over the deformation criteria, this means tendency to tearing points (all FLD Points upper the S minor elongation).

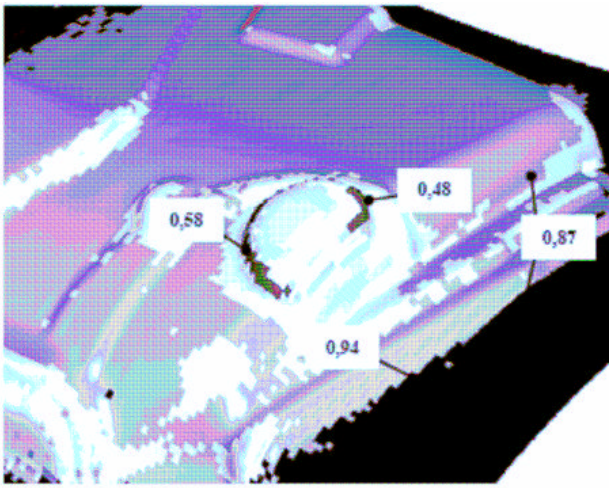

Figure 8. Thickness average distribution after deformation in the phase 2 in [mm].

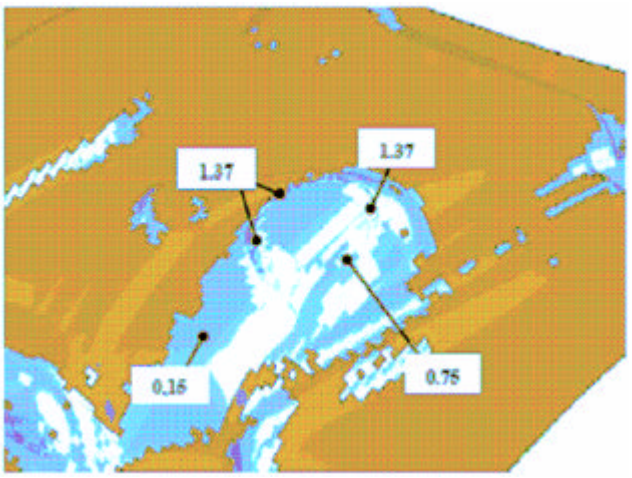

Figure 9. Strain distribution after deformation in the phase 2 for a critical area over the part geometry in reference to the *blank* thickness reduction

According to the established criteria on the topics 2..3.1 and .3.1, the software can determine, from the sheet metal input material data, the limit curve for the FLD criteria, representing on this way the curve limiting the zone 2 (according to the topic 3.1), the criteria for the material tearing. Above the FLC, we have the points where failure occurs and, with a mouse click over these, the software shows over the FE model on which position they occur, showing to the designer engineer the critical points of the part. The inverse can also occur, an element also can be choosing to a point on the FLD. Calculating the dates $(e_{\min}, e_{\max})$ through the equation (35), the program calculates the distribution of points (or the distance to limit curve FLC) for a choosed material, in this case the St1405 in relation to the criteria-limit curve of this. The points over this FLC line therefore are over the established relation of $(e_{\max})$ and will certainly tear (location can be seen on figure 11) for this material and /or for this geometry. Also for elongation visualization over the part, it's also possible to plot a circle distribution over the part surface. On figure 12(a) we have the circle representation at the end of the phase 1 (holder closed) and on the figure 11(b) the circle elongation according to the FLD criteria displayed on the figure 10 for a complete part (end of phase 2).

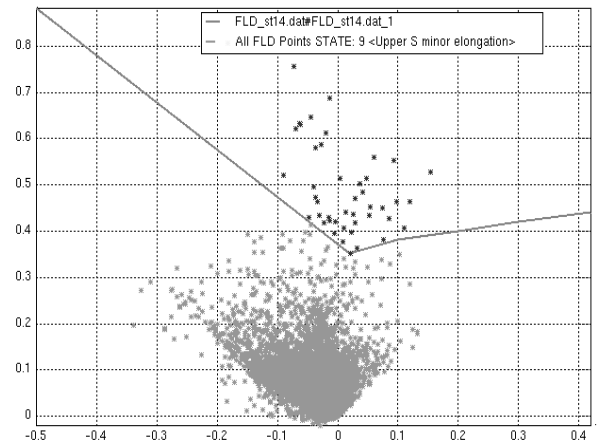

Figure 10. FLD representation, over the FLC (zone 1) are plotted the points over the criteria for the St1405 material according to the quarter panel stamped geometry.

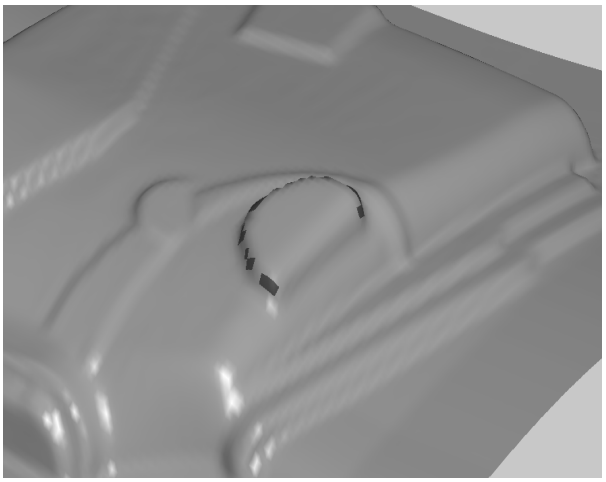

Figure 11. Quarter panel geometry, where we can identify the critical elements represented in the fig. 10 (FLD), on the region above the FLC, zone 1.

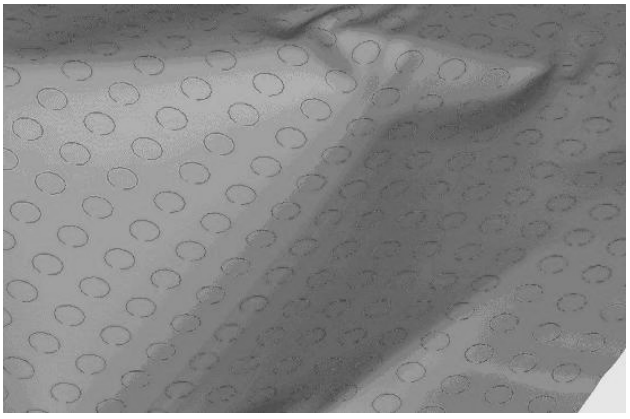

(a)

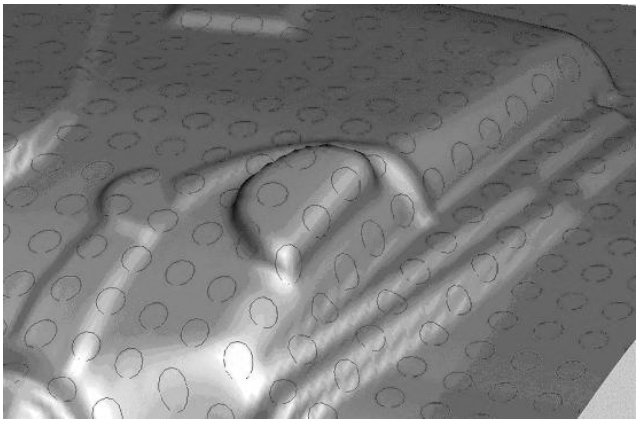

(b)

Figure 12 Grid Circle representation: phase 1 (a) phase 2 (b).

Regarding the results of the calculation the material flow, thickness distribution and failure in the sheet was in good correspondent with the experimental results. The results show that in a comparison between calculated and experienced results (fig.13), in the same critical areas the sheet tearing was founded.

Figure 13. Prototype pressed body-in-white part. It's possible to see that the tearing happened on the same regions as showed on figure 11.

3.4 Tool Optimization

The criteria of a limit shell thickness have been reached, because of the friction coefficient between the punch and the blank has been too high. The modification of the tool geometry on the critical area was recommended after the modifications, a new calculation has been performed. In the critical areas the minimal thickness was calculated to 0,71 mm.

8. CONCLUSIONS

The activities on simulation and design of sheet metal forming tools as well as of sheet metal parts were improved by the use of dynamic explicit FEM modeling. Using the FLD as a design tool, the engineers and designers can check the behavior of certain material families for their stamping applications, according to their standards and applications of the part. The dynamic explicit fem code was able to help the authors to solve a practical example of the automotive industry aimming:

- The plot of a FLD, the FLC and the failure representation (tearing) of the pressed part critical points for a St1405 material,
- Improving the process by optimizing the material flow and the sheet thickness distribution,
- The circle grid representation on a part surface (FEM),
- Calculate equivalent plastic strain and the indication of failure (tearing and wrinkling),

Also working in this way, the sheet metal forming simulation can be used for comparative tool optimization and to study the influence of varying process parameters. With more experience using and improving the practical and theoretical models, sheet forming simulation has become a powerful tool to reduce development time, reduce costs and improve quality.

9. REFERENCES

AZUSHIMA, A.; MIYAMOTO, J.; KUDO, H.; Effect of Surface Topography of Workpiece on Pressure Dependence of Coefficient of Friction in Sheet Metal Forming, Annals of the CIRP, 47, 1, 1998, 479-482

BATALHA, G. F. & STIPKOVIC, M.; Estimation of the Contact Conditions and its Influences on the Interface Friction in Forming Processes, In: Pietrzyk, M. et al. Ed. Metal Forming 2000. Rotterdam: Balkema 2000, 71-78.

BATALHA, G. F. & STIPKOVIC, M.: Quantitative characterization of the surface topography of cold rolled sheets – new approaches and possibilities, J. Material Processing Technology 113, 2001, 732-738.

BERG, H. & HORA, P.; Simulation of sheet metal forming process using different anisotropic constitutive models, Proc. NUMIFORM 98.

DAMOULIS, G. ; BATALHA, G.F.; Development of Industrial Sheet Metal Forming Process Using Computer Simulation as Integrated Tool in the Car Body Development; COBEF 2003
DAMOULIS, G.; BATALHA, G.; SCHWARZWALD, R.; New Trends in Computer Simulation as Integrated Tool for Automotive Components Development, NUMIFORM, Ohio 2003
GOODWIN, G. M.; "Application of Strain Analysis to Sheet Metal Forming Problems in the Press Shop"; La Metalurgia Italiana, no. 8 –1968; pg. 767 a 774.
HAUG E., PASCALE E.DI, PICKETT A.K., ULRICH, D. ESI; Industrial Sheet Metal Forming Simulation Using Explicit FE-Methods, VDI Bericht Nr. 894, Germany 1991
HEATH A., PICKETT A.,ULRICH, D.; Development of Industrial Sheet Metal Forming Process Using Computer Simulation, Dedicated Conference on Lean Manufacturing in Automotive Industries, Aachen, Germany, 1993
HILL, R.; A Theory of the Yielding and Plastic Flow of Anisotropic Metals. Proc. Roy.Soc. A193, 1948
HILL, R.; Constitutive Modeling orthotropic plasticity in sheet metals, J. Mech. Phys. Solids, v. 38, n. 3, 1990, pp. 405, p. 405-17.
KEELER, S. P.; "Determination of Forming Limits in Automotive Stampings", Sheet Metal Industries -September 1965; pg. 357 a 361 e 364.
MAZILIU, L. S. and KURR, J. Anisotropy Evolution by Cold Prestrained Metals Described by ICT-Theory. Journal of Material Processing Technology, Vol.24, pp.303-311, 1990
SWIFT, H. W.; "Plastic Instability under Plane Stress"; Journal of the Mechanical and Physics of Solids, Vol. 1- 1952; pg.1 a 18.

ANALISE DE PROCESSOS DE CONFORMAÇÃO DE CHAPAS METALICAS USANDO O DIAGRAMA LIMITE DE CONFORMAÇÃO (FLD) ATRAVÉS DE SIMULAÇÃO COMPUTACIONAL INTEGRADA NO DESENVOLVIMENTO DE CARROCERIAS AUTOMOTIVAS

Gleiton Luiz Damoulis
Edson Gomes
Gilmar Ferreira Batalha
Laboratório de Engenharia de Fabricação - Escola Politécnica da Universidade de São Paulo – Depto of Mechatronics & Mechanical Systems Engineering - Av. Prof. Mello Moraes, 2231, 05508.970 - S. Paulo, SP - BRAZIL. Fone 00 55 11 30915763 - e-mail: gilmar.batalha@poli.usp.br

Resumo *As exigências de mercado tornam-se mais persistentes através da introdução das novas tecnologias que podem conduzir aos projetos de veículo para alcançar padrões de segurança elevados, redução da massa (melhorias no consumo de combustível, nas emissões e nas tendências do desempenho), dos níveis da qualidade da classe mundial, custos de fabricação e em planejamento da manufatura, novas características de projeto devidas e principalmente da introdução de novos materiais na chamada tecnologia de veiculos de massa reduzida. Uma nova geração de softwares de simulação pelo método de elementos finito explícito ou implícito está tornando-se mais acessível e aumentando sua confiabilidade nos resultados apresentados. A pergunta é, como pode este o software apoiar um coordenador do desenvolvimento de processo e produto na escolha das geometrias dos componentes da carroceria direto do projeto, dimensionamento do blank e da ferramenta, os parâmetros processo, e além disso selecionar o material correto, principalmente devido a introdução de mercado de muitas novas gamas de aços para automóveis, nos últimos anos. Em um exemplo, no desenvolvimento de carroceria automotiva, o projeto dos painéis do corpo pode ser apoiado eficazmente pelo uso do diagrama limite de conformação (FLD), com a simulação de computador do processo de conformação da chapa metálica com o MEF. Este trabalho descreve como um programa de elementos finito explícito aplicado à configuração para o processo de estampagem profunda, realizados pelo uso da metodologia de FLD e do procedimento atualizando para os dados modelo e o processo computacional. A parte principal do papel discute habilidades aplicadas simulação e explica em um exemplo do processo industrial como o uso do diagrama FLD ajuda melhorar a interpretação da simulação e na escolha do melhor aço.*
Palavras-chave*: conformação de chapa, diagrama limite de conformação, simulação, MEF.*